IEEE Open Journal of
Antennas and Propagation

Received 15 January 2021; revised 11 April 2021; accepted 13 April 2021. Date of publication 20 April 2021; date of current version 23 April 2021.

Digital Object Identifier 10.1109/OJAP.2021.3074290

18 Element Massive MIMO/Diversity 5G Smartphones Antenna Design for Sub-6 GHz LTE Bands 42/43 Applications

NAVEEN JAGLAN [1], SAMIR DEV GUPTA [1], AND MOHAMMAD S. SHARAWI [2,3] (Senior Member, IEEE)

[1]Department of Electronics and Communication Engineering, Jaypee University of Information Technology, Waknaghat 173234, India

[2]Electrical Engineering Department, Polytechnique Montréal, Montréal, QC H3T 1J4, Canada

[3]Poly-Grames Research Center, Polytechnique Montréal, Montréal, QC, H3T 1J4 Canada

CORRESPONDING AUTHOR: N. JAGLAN (e-mail: naveenjaglan1@gmail.com)

ABSTRACT This work presents an 18 element antenna system compatible with massive multiple input multiple output (MIMO)/Diversity fourth/fifth generation (4G/5G) smartphones. The antennas are designed at sub-6 GHz long term evolution (LTE) band 42 (3.4-3.6 GHz) and LTE band 43 (3.6-3.8 GHz). A simple slot type antenna is considered as the radiating element, with open ended slots used for obtaining a compact design. These slots also act as decoupling elements to improve the isolation among different radiators. The proposed antenna elements are designed on a low-cost FR-4 substrate having dimension of 150 mm × 80 mm × 1.6 mm, which can be typically used for 6-inch smart phones. The simulated and measured values of antenna gain are found to be greater than 5.3 dBi. Simulated and measured results of the proposed design show excellent impedance matching (reflection coefficient>20 dB), port isolation (>20 dB), total efficiency (>87%) and Envelope Correlation Coefficient (<0.01) over the operating frequency. MIMO antenna performance metrics are verified by calculating the ergodic channel capacity with Kronecker channel model.

INDEX TERMS 5G smartphones, open ended slots, MIMO antennas, massive MIMO, sub-6 GHz band.

I. INTRODUCTION

AS THE world is now moving towards 5G communication systems, the demand for 5G smartphones and 5G base stations [1] will increase exponentially in the coming years. Low order MIMO systems like 2×2 and 4×4 are quite popular for fourth generation (4G) smartphones operating in LTE bands [2]. However, with low order MIMO systems the values of parameters like ergodic channel capacity, spectral efficiency and signal to noise ratio (SNR) can still be increased to meet application and customer demands [3]. 5G communication systems demand better link reliability and data rates of around 1000 times compared to 4G [4]. Low order MIMO systems will not be able to meet these requirements and hence moving to massive MIMO is a possible solution. Even for 4G, having more antenna elements will reduce the effect of blocking some elements by the user hands and thus degrading the link performance. Massive MIMO can increase the spectral efficiency, channel capacity and link reliability to a large extent compared to low order MIMO antennas [5]. A lot of focus of researchers working in 5G communication around the world is on frequency range 1 (FR-1) that includes sub 6 GHz frequency band. In the millimetre wave bands (FR-2), antenna arrays are used with beamforming capabilities. In Sub-6 GHz bands most of the research is focusing on the LTE band 42 and LTE band 43 because these bands are included in 5G communication spectrum in most countries.

Using multi antenna systems for 5G antennas can improve spectral efficiency and channel capacity however integrating massive MIMO antennas in a limited space in the smartphone is a very challenging task. The isolation among the antenna elements must be greater than 15 dB to obtain the best MIMO performance [6]. In recent years, researchers around the world proposed several techniques to improve the isolation among antenna elements. Numerous decoupling structures like extended ground plane [7], electromagnetic

band gap structures [8], parasitic elements [9], T-shaped slots [10] and neutralization lines [11]. The problem with some of these decoupling structures is that the total antenna efficiency decreases. Several other methods to improve the isolation like shown in [12], [13], [14], [15], asymmetrical mirrored antennas [16], [17], self-isolated antenna design methods [18], orthogonal mode pairs [19] and with isolating stub and shorting strip [20] are also proposed by various researchers. In [21], an 8-element MIMO antenna is presented that covers LTE band 42. The measured values of channel capacity are found to be around 16 bps/Hz with 20 dB Signal to Noise Ratio (SNR). However, this design requires a lot of space. In [22], a 10-antenna array for MIMO operation is designed to work in the LTE bands 42/43. The measured value for channel capacity at 20 dB SNR was 47 bps/Hz. In [23], an 8 × 8 MIMO antenna system is proposed to work at 2.6 GHz, 20 dB SNR with ergodic channel capacity of 40 bps/Hz. If the MIMO antenna is designed irrespective of any external decoupling arrangement, the isolation of the design can be increased without compromising the total efficiency. However, this is still a challenge to increase the number of antenna elements with acceptable level of isolation and efficiency so as to achieve better ergodic channel capacity.

In this paper an 18 element massive MIMO antenna is designed without the help of any external decoupling structures for handheld devices. Compact single antenna slot-based elements are chosen. The antenna is designed to work in LTE band 42 and LTE band 43 that can be used in 5G smartphones. The isolation among the antenna elements is found to be greater than 20 dB and total efficiency obtained to be more than 87%. The maximum value of ergodic channel capacity at 20 dB SNR reaches upto 81 bps/Hz. To achieve good isolation among antenna elements, open ended slots are used in the ground plane. All 18 elements are properly arranged on the ground plane and space is also provided for 2G/3G/4G antennas. The proposed design is simulated, fabricated and tested.

II. DESIGN OF PROPOSED MIMO ANTENNA

Fig. 1(a) shows the layout of the proposed massive MIMO antenna. It has 18 antenna elements numbered from Ant 1 to Ant 18. These antenna elements are designed on an FR-4 substrate (with relative permittivity value of 4.4 and loss tangent of 0.02) with copper cladding on both sides. The substrate used in the design has a dimension of 150 mm × 80 mm × 1.6 mm that can be used in 6-inch 5G smartphones. This type of substrate is usually termed as printed circuit board (PCB) as on the top surface antenna feed line is there with yellow color and on the bottom surface ground plane is with green color. Ant 17 and Ant 18 are placed horizontally along the shorter edges and Ant 1 to Ant 16 are placed vertically along the longer edges. The white coloured rectangular space on the shorter edges is set aside for accommodating 2G/3G/4G antennas. Fig. 1(b) shows the comprehensive design of an individual slot antenna element. A simple and

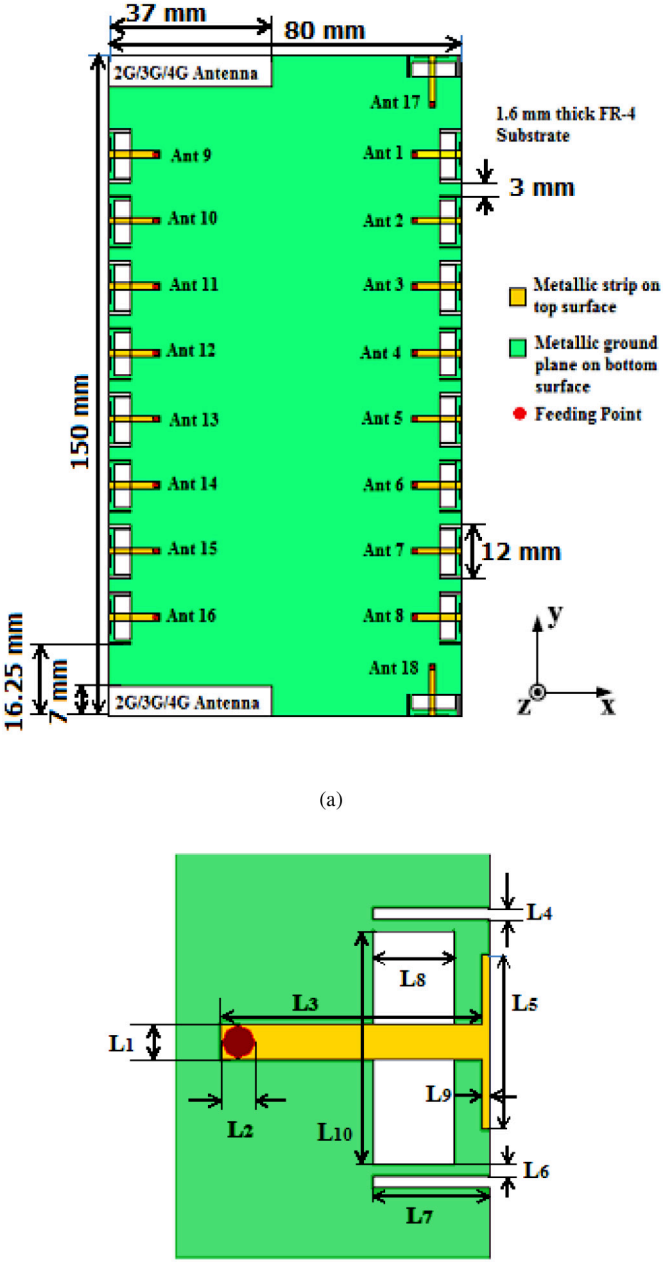

FIGURE 1. (a) Design of proposed 18 element MIMO antenna with detailed dimensions, (b) Detailed view of single slot antenna with decoupling open ended slots.

efficient way of reducing the mutual coupling among the closely spaced antenna elements is presented. Two open ended slots of the same dimensions with width of 0.5 mm and length of 5 mm are used. A rectangular slot radiator in the ground plane with dimensions of 10 × 3.5 mm^2 is fed using a T-shaped feeding line at the feeding point. It is observed that T-shaped feeding line provides better impedance matching and best radiation efficiency value. The modelling and simulation of the design were carried out using HFSS version 17. Antenna element 1(Ant 1) is shown with two open ended decoupling strips. All the remaining antennas also have the same configuration and dimensions. The dimensions of antenna 1 with open ended decoupling slots are

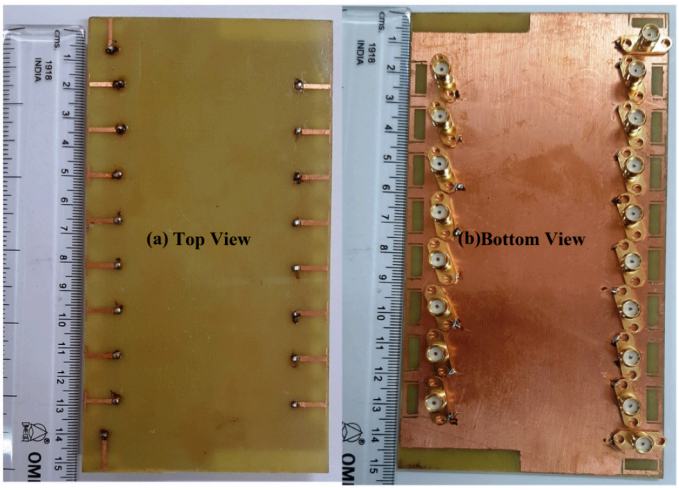

FIGURE 2. Photographs of fabricated design (a) Top view, (b) Bottom view.

given as $L_1 = 1.5$ mm, $L_2 = 1.4$ mm, $L_3 = 11.2$ mm, $L_4 = 0.5$ mm, $L_5 = 7.5$ mm, $L_6 = 0.5$ mm, $L_7 = 5$ mm, $L_8 = 3.5$ mm, $L_9 = 0.3$ mm and $L_{10} = 10$ mm. Firstly, a T-shaped 50 ohm feeding line is designed, then a slot in the ground plane with length of L_{10} and width of L_8 is made. The resulting slot antenna is optimized for best value of radiation efficiency and antenna gain. Open ended rectangular slots with length L_7 and width L_4 are used to minimize the mutual coupling among the antenna elements. The spacing among different antennas is 3 mm. All antenna elements are designed to work in LTE band 42 and LTE band 43.

The proposed slot antenna design is compact having dimensions of 5 mm $\times$ 12 mm and therefore quite suitable for narrow frame 5G smartphones. The proposed antenna design is fabricated. The top and bottom sides of fabricated sample are presented in Fig. 2(a) and 2(b). All 18 ports are fed with 50 ohm SMA connectors through the ground plane.These connectors can easily fed all antenna elements after properly adjusting them on the ground plane.

The simulated current distribution on the antenna structure is shown in Fig. 3. In Fig. 3(a) and Fig. 3(b), current distributions is given when Ant 1 and Ant 13 are excited independently. It can be clearly seen from both the figures that when either of the antennas are excited, the corresponding current do not spread and hence minimizes the coupling with adjacent elements.

Fig. 3(c) shows the surface current distribution on the slotted ground plane of the proposed antenna structure. It can be seen that a strong current flow along the shorter dimension of the slot. The currents flowing along the larger dimensions of the slot are in the opposite direction and thereby reducing the resultant current along this side. Electric field is having the peak in the centre on larger dimension of the slot. Thus the Electric field distribution with in the slot and the current that travels along around the slot perimeter, both contributes to the radiation. Thus, the slot behaves as a resonant radiator at the required frequency band.

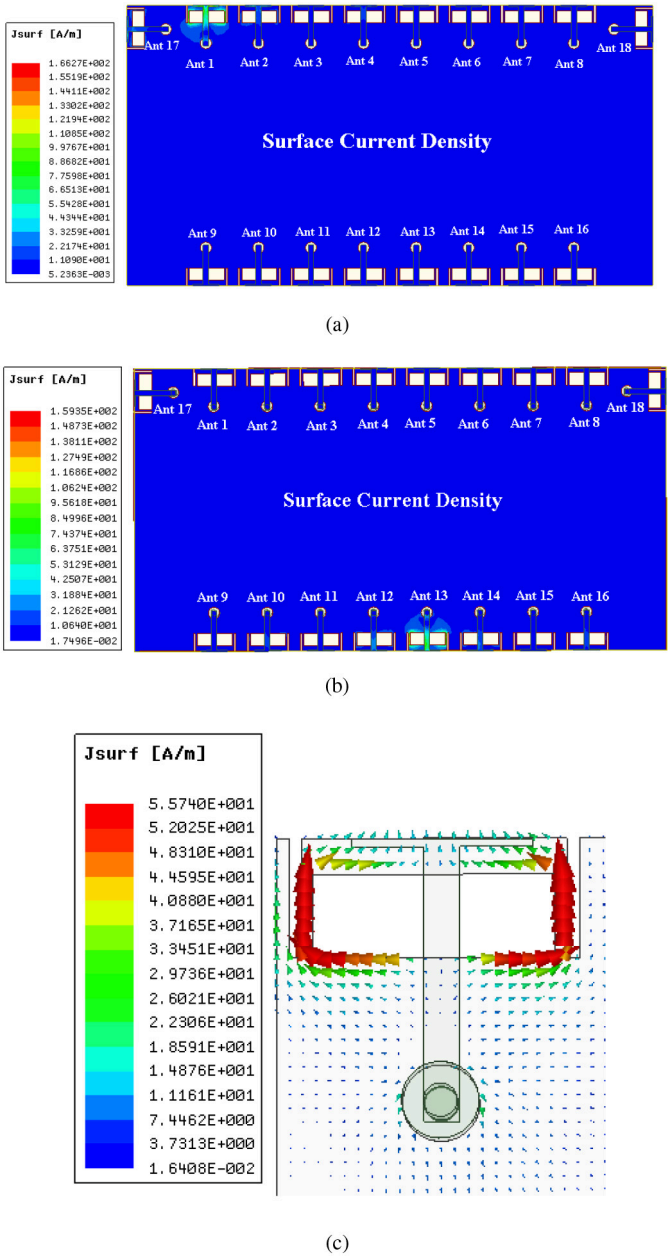

FIGURE 3. Surface electric current distribution on the antenna ground plane at 3.6 GHz when (a) Ant 1 is excited and, (b) Ant 13 is excited, (c) vectored surface current distribution on antenna elements.

III. RESULTS AND DISCUSSION

A. SCATTERING PARAMETERS, EFFICIENCY AND RADIATION PATTERNS

Simulated curves of the reflection coefficients for Ant 1 to Ant 8 and Ant 18 are given in Fig. 4(a). Fig. 4(b) shows the simulated reflection coefficients of Ant 9 to Ant 16 and Ant 17. It can be observed that the magnitude of the reflection coefficient for all the antennas is greater than 20 dB in LTE band 42 and 43. All antennas are identical in the proposed design hence the reflection coefficient values remain almost the same. While obtaining the reflection coefficient for a single element the other antennas are terminated with 50 ohm.

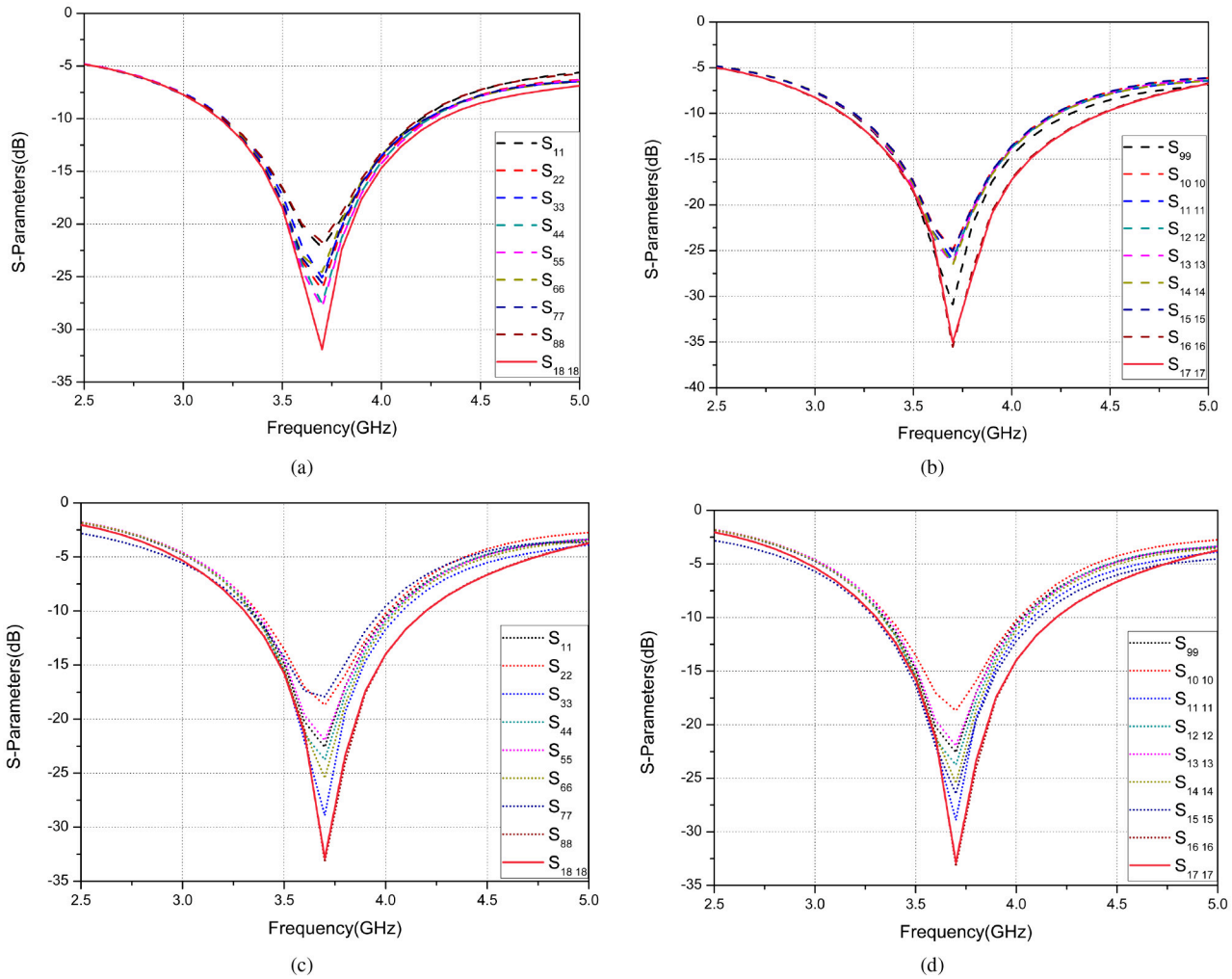

FIGURE 4. **(a) Simulated reflection coefficient values for Ant 1 to Ant 8 and Ant 18, (b) Simulated reflection coefficient values for Ant 9 to Ant 16 and Ant 17, (c) Measured values of reflection coefficients for Ant 1 to Ant 8 and Ant 18, (d) Measured values of reflection coefficients for Ant 9 to Ant 16 and Ant 17.**

Measured values of reflection coefficients for Ant 1 to Ant 8 and Ant 18 are given in Fig. 4(c) to validate the simulated results. In Fig. 4(d) measured reflection coefficients for Ant 9 to Ant 16 and Ant 17 is shown. It can be concluded that all 18 antenna elements have proper impedance matching and are placed perfectly without affecting the refection coefficient of neighbouring antenna elements.

The -10 dB measured bandwidth for all antennas is more than 900 MHz. The simulated and measured curves of port coupling (S_{xy}) are shown in Fig. 5(a) and Fig. 5(b) respectively. It can be observed easily that the magnitude of isolation is greater than 20 dB for all possible combinations. The geometry of the antenna and open ended decoupling slots are optimized so that the mutual coupling can be reduced to a large extent.

The antenna elements are arranged orthogonally to reduce the ground plane effects which helps in improving the isolation among antenna elements. The simulated and measured curves of coupling among different antenna ports are shown in Fig. 6(a) and Fig. 6(b) respectively. The results of maximum antenna pairs are considered that help in achieving excellent diversity and multiplexing performance. The measurements of the S-parameters were done with an *Agilent* Network Analyzer PNA-L series. The antenna efficiency and radiation patterns were measured using a microwave shielded far-field anechoic chamber.

The envelope correlation coefficient (ECC) and ergodic channel capacity are determined using the measured patterns and results. As all antenna elements are identical and the measured and simulations results shows good agreement. The small deviations may be attributed to fabrication and measurement inaccuracies. The measurement set up of the proposed antenna is shown in Fig. 7. The Fig. 8(a) and Fig. 8(b) represents the variation of simulated and measured values of antenna gain with frequency for different antenna elements.It can be seen that the value of gain is greater than 5.3 dBi for all antenna elements.

In Fig. 9(a) simulated values of antenna efficiencies are shown for Ant 1 to Ant 8 as well as Ant 17 and Ant 18.

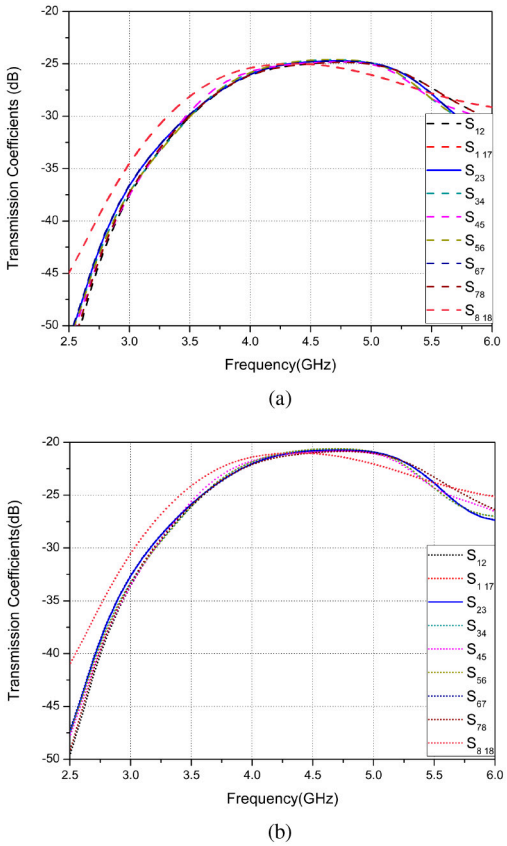

FIGURE 5. (a) Simulated values of mutual coupling among different antenna element pairs, (b) Measured values of mutual coupling among different antenna element pairs.

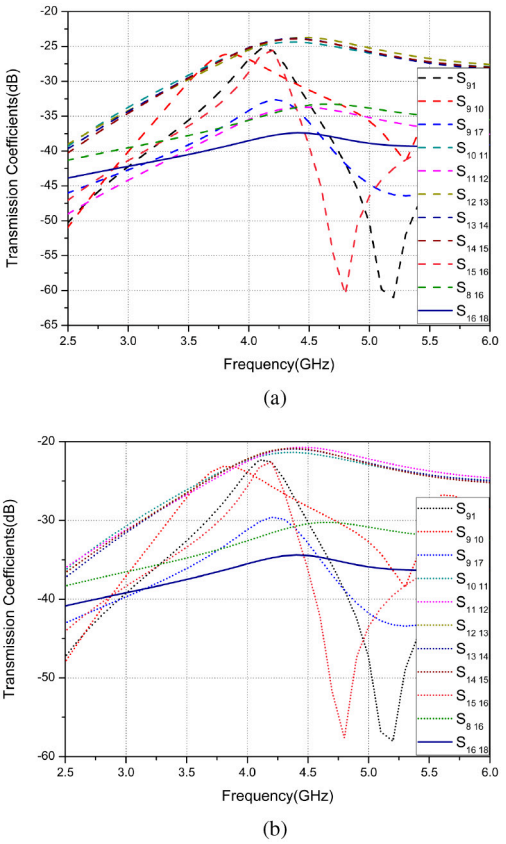

FIGURE 6. (a) Simulated values of mutual coupling among different antenna element pairs, (b) Measured values of mutual coupling among different antenna element pairs.

Fig. 9(b) shows the measured values of total efficiencies for Ant 1 to Ant 8 as well as Ant 17 and Ant 18.

Fig. 10(a) shows the simulated antenna efficiencies for Ant 9 to Ant 16. Fig. 10(b) shows the measured antenna efficiency for Ant 9 to Ant 16. It is observed that the simulated and measured efficiencies of all elements are greater than 87% over the complete band of operation. The measured values of radiation efficiency are within the limits required for mobile communication [24].

B. DIVERSITY AND MULTIPLEXING PARAMETERS

The important parameters of MIMO antennas such as ECC and ergodic channel capacity are evaluated in this section. ECC gives the value of correlation between radiation patterns of two radiators in any MIMO antenna system. ECC is considered as the most significant parameter for calculation of diversity gain of MIMO antennas. ECC values below 0.5 shows good diversity performance for 5G MIMO systems [25]. When the value of ECC is greater than 0.5 then the correlation among antenna elements and channel paths is high and hence the performance of MIMO antenna

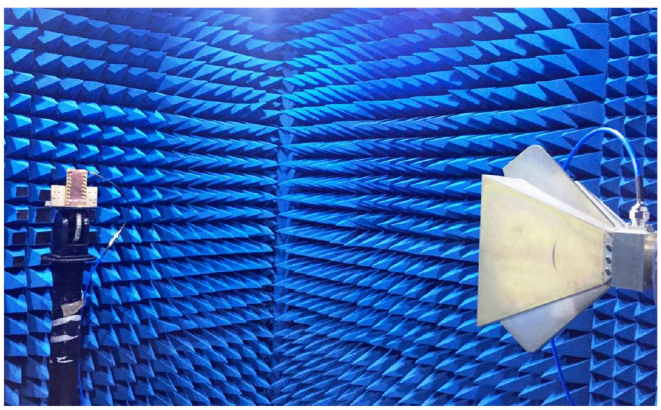

FIGURE 7. Measurement set up of the proposed antenna in anechoic chamber.

$$\rho_{ij} = \left| \frac{\int_0^{2\pi}\int_0^{\pi}(XPR.E_{\theta i}.E^*_{\theta j}.P_\theta + XPR.E_{\phi i}.E^*_{\phi j}.P_\phi)\sin(\theta)d\theta d\phi}{\sqrt{\prod_{k=i,j}\int_0^{2\pi}\int_0^{\pi}(XPR.E_{\theta k}.E^*_{\theta k}.P_\theta + XPR.E_{\phi k}.E^*_{\phi k}.P_\phi)\sin(\theta)d\theta d\phi}} \right|^2 \quad (1)$$

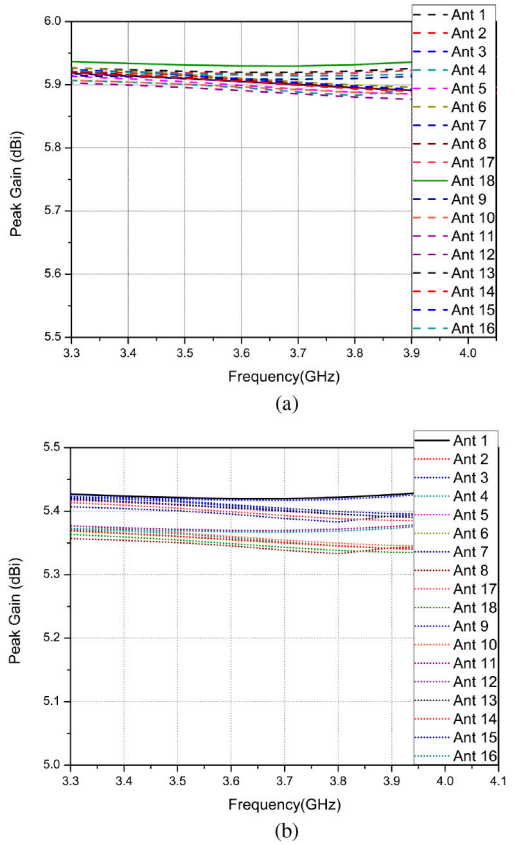

FIGURE 8. (a) Variation of simulated values of antenna gain with frequency for different antenna elements, (b) Variation of measured values of antenna gain with frequency for different antenna elements.

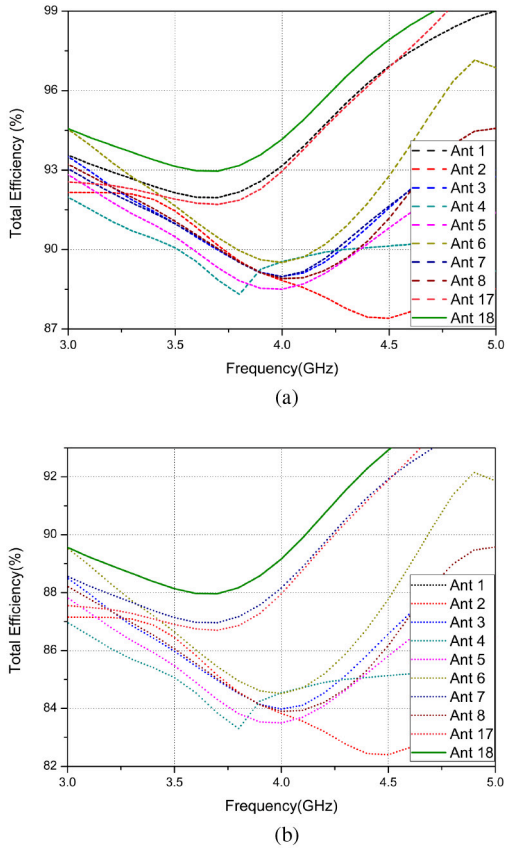

FIGURE 9. (a) Simulated antenna efficiency values for Ant 1 to Ant 8 as well as Ant 17 to Ant 18, (b) Measured antenna efficiency values for Ant 1 to Ant 8 as well as Ant 17 and Ant 18.

deteriorates. The reason is that MIMO systems work best when independence between the received signals is achieved in order to offer excellent diversity and sovereign channels in spatial multiplexing. ECC among Ant i and Ant $j(\rho_{ij})$ is calculated using far field radiation patterns by following expressions [25] as:

Here XPR is the cross polarization ratio of vertical and horizontal polarized components, $E_{\theta i}$, $E_{\theta j}$, $E_{\phi} i, E_{\phi j}$ are the far-field components of antenna elements, where θ and ϕ in the subscript denotes the vertical and horizontal polarizations. P_{θ} and P_{ϕ} represents are angular power spectrum of the propagation environment which satisfies the following conditions:

$$\int_0^{2\pi}\int_0^{\pi} P_{\theta}.\sin(\theta)d\theta d\phi = 1 \tag{2}$$

$$\int_0^{2\pi}\int_0^{\pi} P_{\phi}.\sin(\theta)d\theta d\phi = 1 \tag{3}$$

Therefore ECC is calculated using the three dimensionally distributed complex electric field values considering the assumption that the propagation channel is uniform and the incident isotropic field is distributed in theta-polarized and phi-polarized directions [26]. Fig. 12 shows the calculated ECC among different antenna elements calculated using radiation patterns. Both simulated and measured values of ECC are found to be less than 0.01 over both LTE band 42 and LTE band 43. The measured value of ECC for proposed design is extremely less than the mandatory value of 0.5 for 5G MIMO array.

The instantaneous channel capacity assuming M $\times$ M MIMO channel H, without any channel knowledge at the transmitter side is given by [24].

$$C = \log_2\left(I_m + \frac{\rho_T}{M}HH^H\right) \tag{4}$$

where C denotes channel capacity, I_m denotes identity matrix, ρ_T is Signal to Noise ratio which is given by $\rho_T = \frac{P_T}{\sigma_N^2}$. P_T denotes power transmitted and σ_N^2 denotes the noise power at receiver side. In antenna design, independent and identically distributed (*i.i.d.*) Rayleigh fading channel H_w is considered as reference propagation environment. The values of H_w are zero mean circular symmetric complex Gaussian random variables. If the case of receiving antenna is considered, the MIMO channel is given as:

$$H = R^{1/2}H_w \tag{5}$$

TABLE 1. Comparison of performance of different 5G antenna arrays.

References	Bandwidth (GHz)	S_{ij} (dB)/ECC	Total Efficiency (%)	Peak Channel Capacity (bps/Hz,20dB SNR)
Proposed	3.3-3.8 (-10dB)	<-20/0.01	87-93	81(18×18).
[11]	3.4-3.6 (-10dB)	<-10/0.2	62-78	40(8×8).
[16]	3.4-3.6 (-6dB)	<-10/0.1	40-60	36(8×8).
[18]	3.4-3.6 (-10dB)	<-19.1/0.012	59-68	Not Given(8×8).
[19]	3.4-3.6 (-6 dB)	<-17/0.07	49-61	Not Given (8×8).
[22]	3.4-3.8 (-10dB)	<-10/0.1	42-62	47 (10×10).
[28]	3.4-3.6 (-10dB)	<-17.5/0.05	62-76	40.8(8×8).
[29]	3.4-3.6 (-10dB)	<-17/0.1	>58	19 (4×4).
[30]	3.4-3.6 (-10dB)	<-16/0.05	50-75	39.8(8×8).
[31]	3.4-3.6 (-6dB)	<-12.7/0.13	39-50	Not Given (4×4).
[32]	3.4-3.6 (-6dB)	<-10/0.32	40-60	70 (16×16).

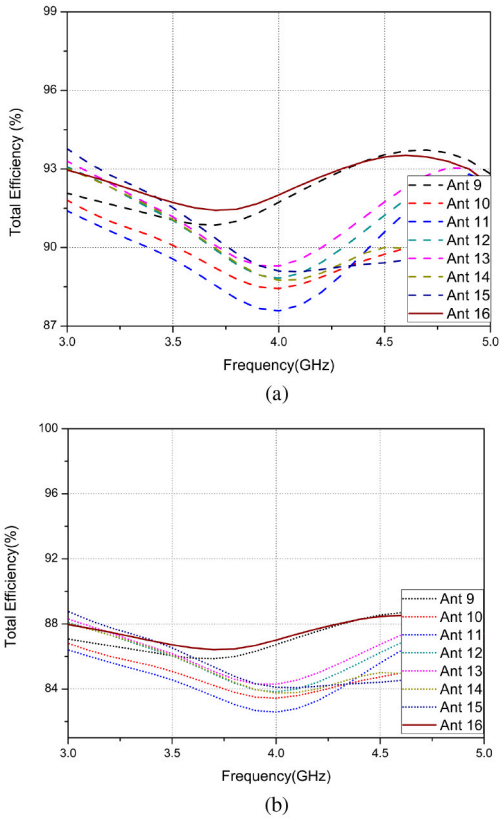

FIGURE 10. (a) Simulated values of antenna efficiency for Ant 9 to Ant 16, (b) Measured values of antenna efficiency for Ant 9 to Ant 16.

R is received correlation matrix that describes the efficiency, efficiency imbalance and correlation among receiving antennas. MIMO performance is usually described by ergodic channel capacity [27] which is basically obtained from a large number of Monte Carlo realizations of channel matrix H and is given by following expression:

$$C = E\left(\log_2\left(I_m + \frac{\rho_T}{M} HH^H\right)\right) \tag{6}$$

Ergodic channel capacity [27] is calculated with MATLAB using Kronecker channel model by averaging 100,000 i.i.d. Rayleigh fading channel realizations in Fig. 12. It is assumed that transmitter has no channel state information and 20 dB SNR is considered at receiver. The ergodic channel capacity of the proposed MIMO antenna system fluctuates between 77.1 bps/Hz and 81 bps/Hz. The peak realizable channel capacity of (81 bps/Hz) is 78.3% of the upper theoretical limit of an 18 × 18 MIMO system which is (103.5 bps/Hz) and is 704.34% of the maximum bounds for a typical 2 × 2 MIMO system (11.5 bps/Hz), thus excellent multiplexing competency can be achieved.

C. DETAILED COMPARISON WITH DIFFERENT 5G HANDSET MIMO ARRAYS

Table 1 shows a detailed comparison of the proposed work and other published ones. Most recent publications have been added in the comparison table so as to highlight the advantages of our proposed antenna over others. The advantage of the proposed antenna is that it has isolation levels better than 20 dB, ECC (<0.01), total efficiency higher than 87% and peak channel capacity of 81 bps/Hz. The proposed antenna shows improvement in almost all parameters used to evaluate MIMO performance. The proposed 18 element antenna array has the advantage of superior performance and hence can be considered for future 5G smartphones applications.

D. USER'S HAND GRIP IMPACT

The effect of human hand grip effect is analysed in this section. A hand held smartphone is considered in two different situations [2] specifically Single Hand Mode (SHM) and Double Hand mode (DHM). Two representations of hand held smartphone in SHM and DHM are given in Fig. 14. The impact of the human head is not analysed as massive MIMO system for sub-6 GHz band is mainly used for data transmission as compared to talk mode.

For SHM, Ant 1 to Ant 4 as well as Ant 9 to Ant 11 are in contact to the fingers and hence this mode effects the reflection coefficient to a large extent. The reflection coefficient variations with frequency for SHM is shown in Fig. 15.

Minor variation in the reflection coefficients of other antenna elements is observed. In Fig. 16 coupling among the different antenna ports in SHM is shown. It can be observed that the isolation among the antenna elements are higher than 20 dB across the whole operating bandwidth.

In addition, the peak ergodic channel capacity of the proposed MIMO antenna system with SHM and DHM are

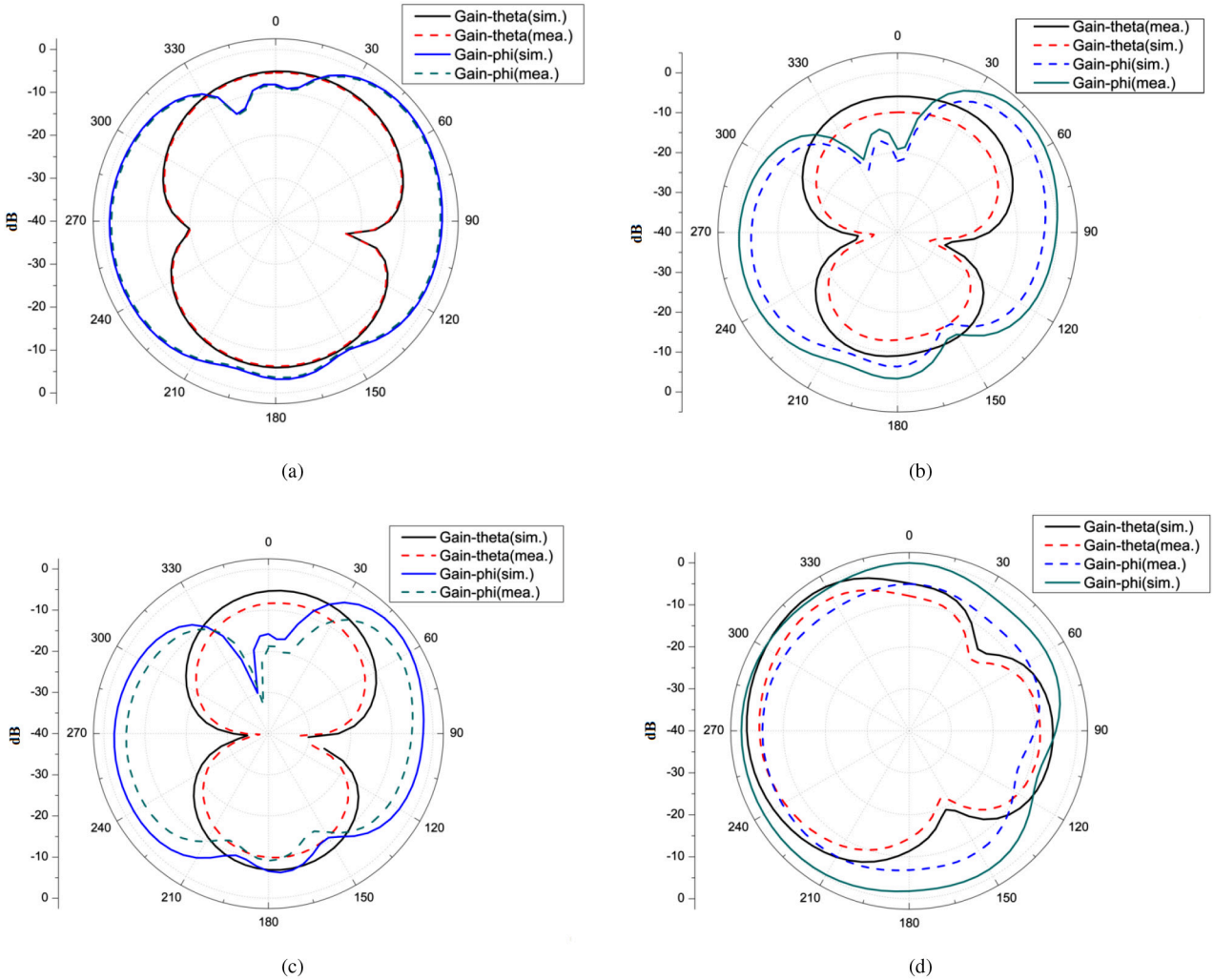

FIGURE 11. Simulated and Measured radiation patterns at 3.6 GHz of (a) Ant 1 (b), Ant 3, (c) Ant 7, (d) Ant 17.

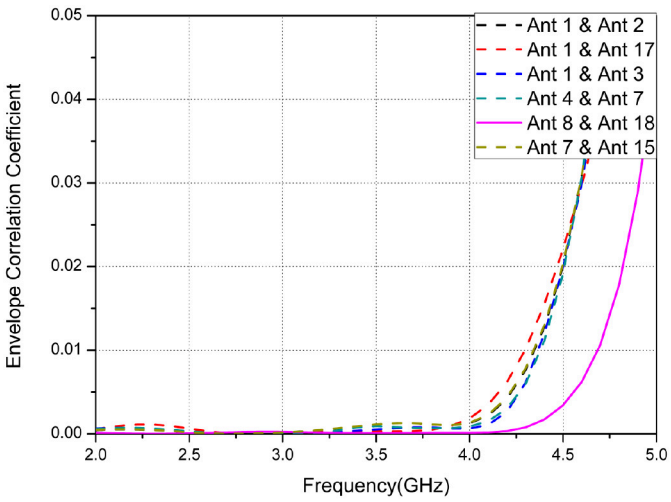

FIGURE 12. Calculated value of ECC for various antenna pairs.

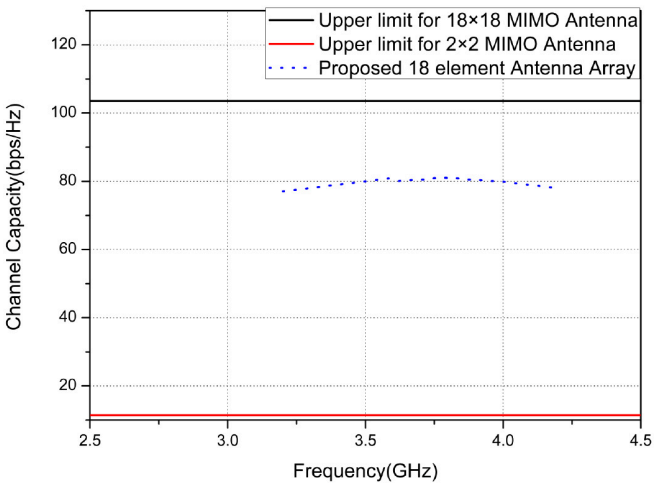

FIGURE 13. Calculation of ergodic channel capacity from measured values.

found to be 40.75 bps/Hz and 55.3 bps/Hz respectively and is shown in Fig. 17. When some of the antenna elements are blocked by user's hand the peak channel capacity of the proposed antenna is decreased. However, the performance of the proposed antenna can be considered satisfactory even under the influence of human hand grip. The proposed

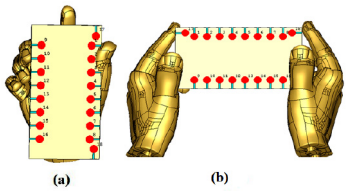

FIGURE 14. Two different representations of a handheld smartphone (a) Single Hand Mode (SHM), (b) Dual Hand Mode (DHM).

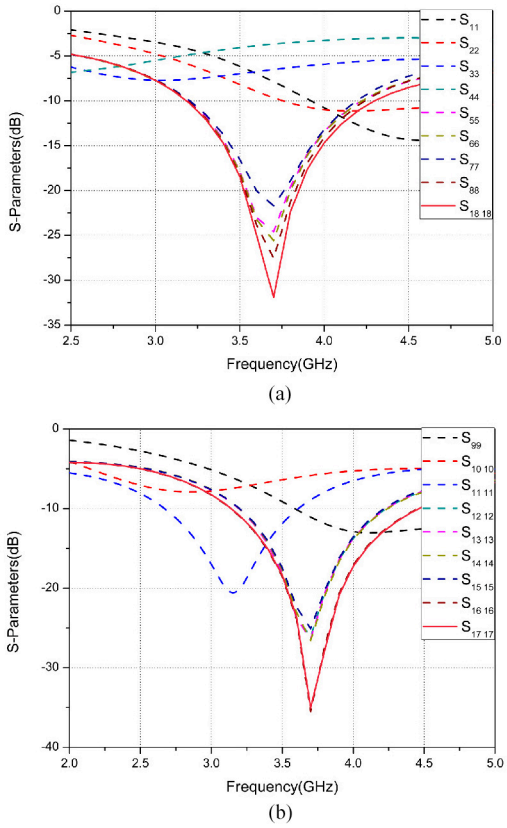

FIGURE 15. Simulated reflection coefficients in SHM (a) Ant 1 to Ant 8 and Ant 18, (b) Ant 9 to Ant 17.

MIMO system can be considered as a robust design for innovative 5G smartphones.

Further, in Fig. 18 the total efficiency of different antenna elements is shown. The total efficiency for Ant 1 to Ant 4 and Ant 9 to Ant 11 is reduced to below 20% due to hand effect, as expected. The same behaviour is seen for the DHM where Ant 9, 16, 17 and 18 are blocked.

In Fig. 19 shows the reflection coefficients of antenna elements in DHM. It can be seen that Ant 9, Ant 16, Ant 17 and Ant 18 are in direct contact with user hands and hence have distorted values of reflection coefficients.

Fig. 20 shows the transmission coefficients of different antenna pairs. The isolation among different antenna elements in DHM is found to be greater than 20 dB.

Fig. 21 shows the simulated total efficiency for DHM. Due to absorption of power by hand tissues the total efficiency for Ant 9, Ant 16, Ant 17 and Ant 18 are reduced to below 20%.

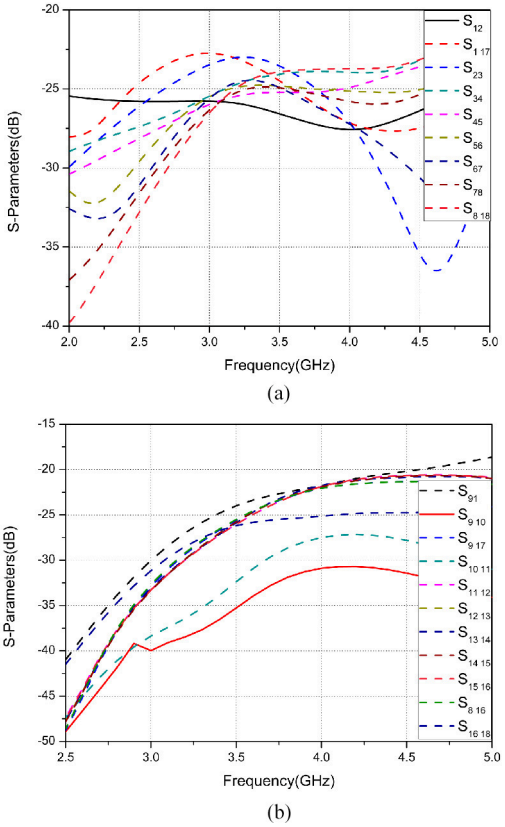

FIGURE 16. (a), (b) Simulated transmission coefficients in SHM for different antenna pairs.

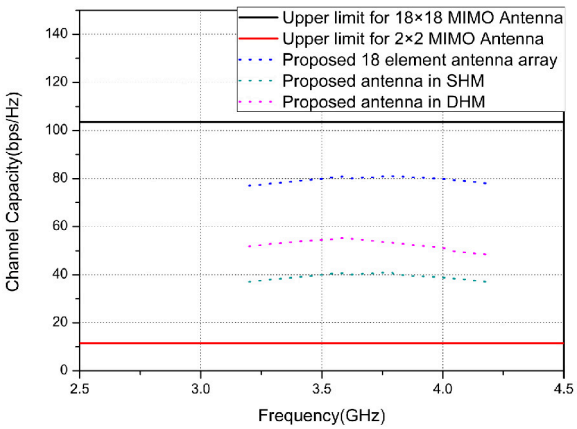

FIGURE 17. Calculation of ergodic channel capacity from measured values considering hand effect.

E. IMPACT OF SMARTPHONE BATTERY

We have investigated the proposed antenna characteristics with a metal block of size 118 mm × 40 mm × 4mm which can be assumed equivalent to a battery. This metal block is placed over the front surface of PCB and is connected to the ground with the help of 16 electrically conducting shorting pins as shown in 22(a). It is observed that battery will have negligible impact on the radiation performance of the antenna elements. It can be seen

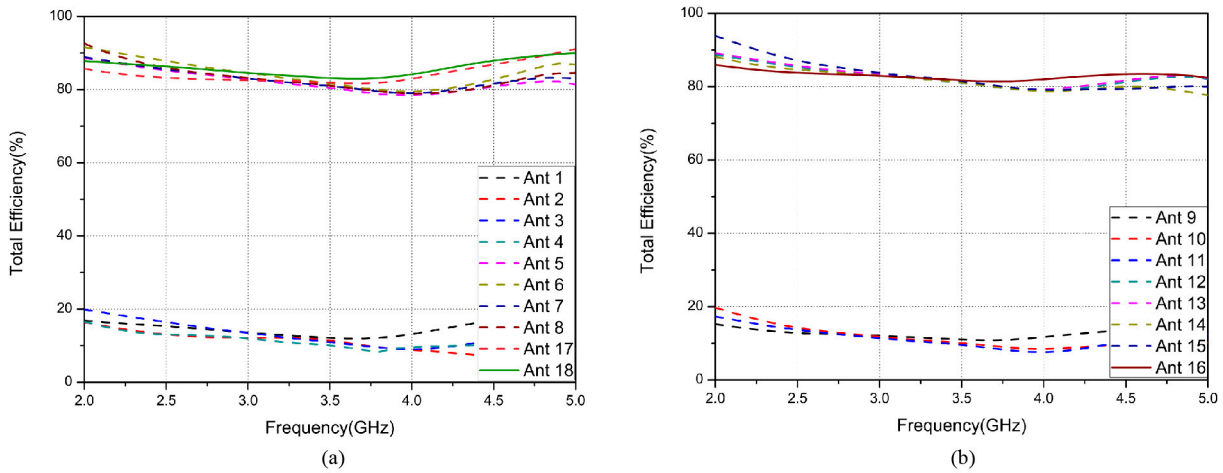

FIGURE 18. Simulated values of total efficiency in SHM for (a) Ant1 to Ant 8 and Ant 17 to Ant 18, (b) Ant 9 to Ant 16.

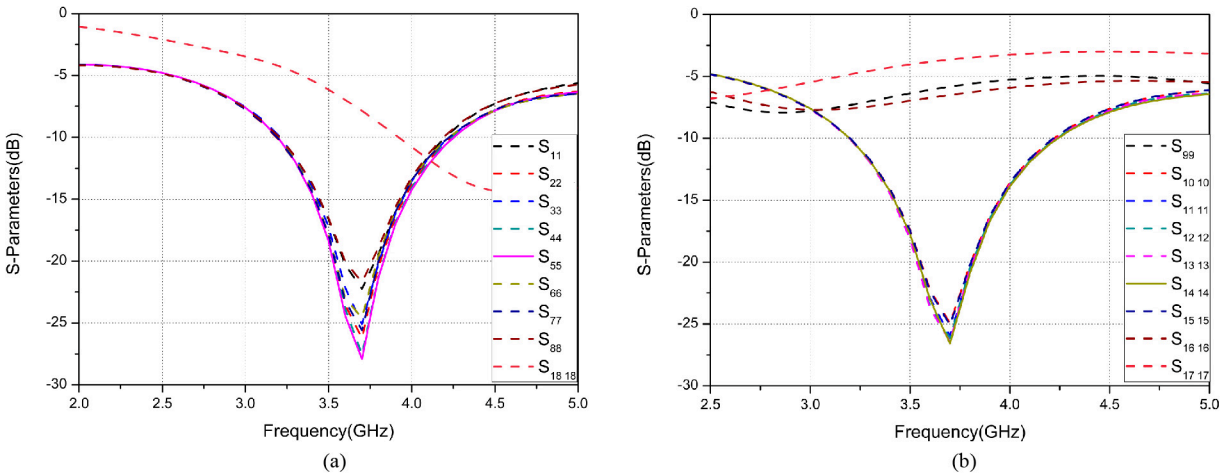

FIGURE 19. Simulated reflection coefficients in DHM (a) Ant 1 to Ant 8 and Ant 18, (b) Ant 9 to Ant 17.

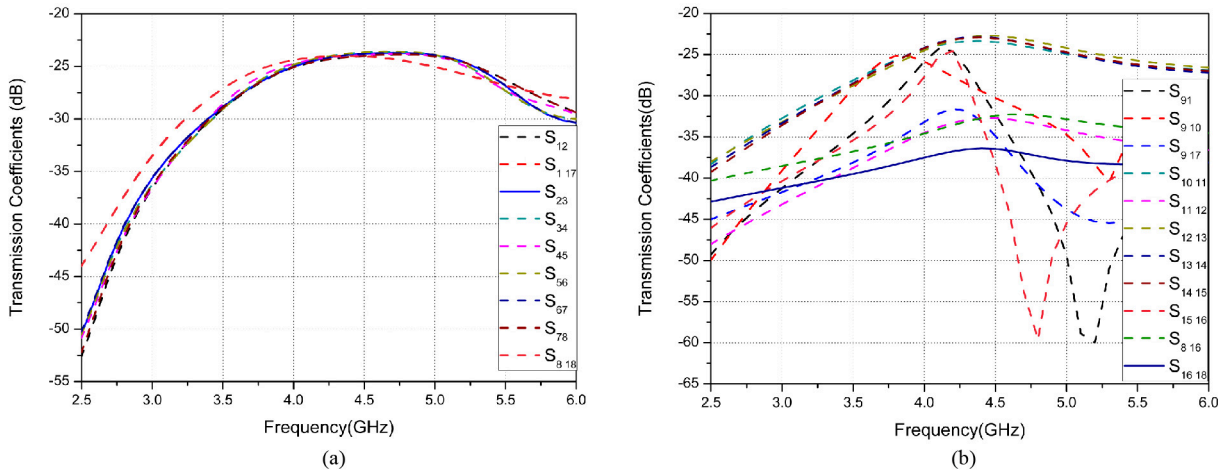

FIGURE 20. (a), (b) Simulated transmission coefficients in DHM for different antenna pairs.

from simulated results given in Fig. 22(b) that even after placing the battery the magnitude of reflection coefficients is greater than 10 dB for complete operating frequency range. Fig. 23 shows that there is minor variation in the total efficiency of antenna elements after placement of battery.

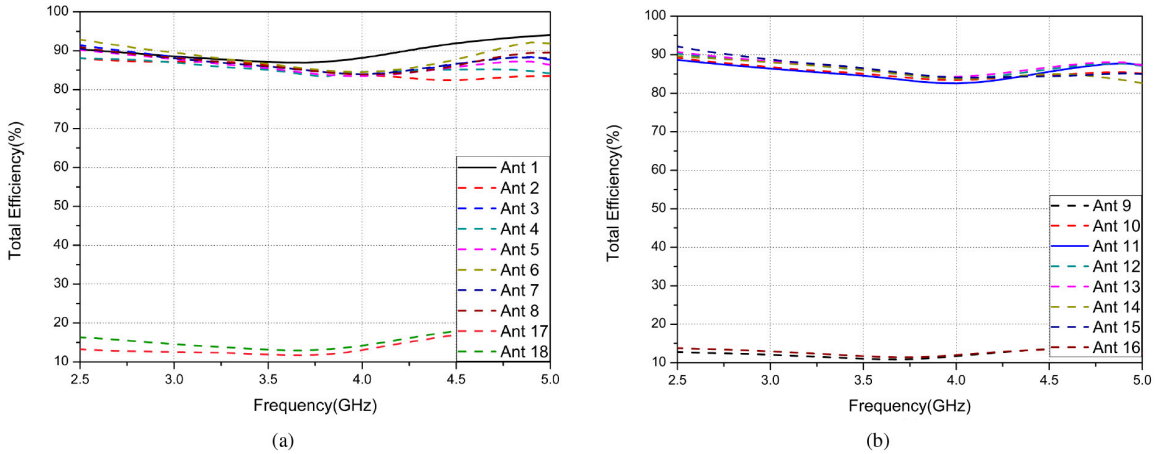

FIGURE 21. Simulated values of total efficiency in DHM for (a) Ant1 to Ant 8 and Ant 17 to Ant 18, (b) Ant 9 to Ant 16.

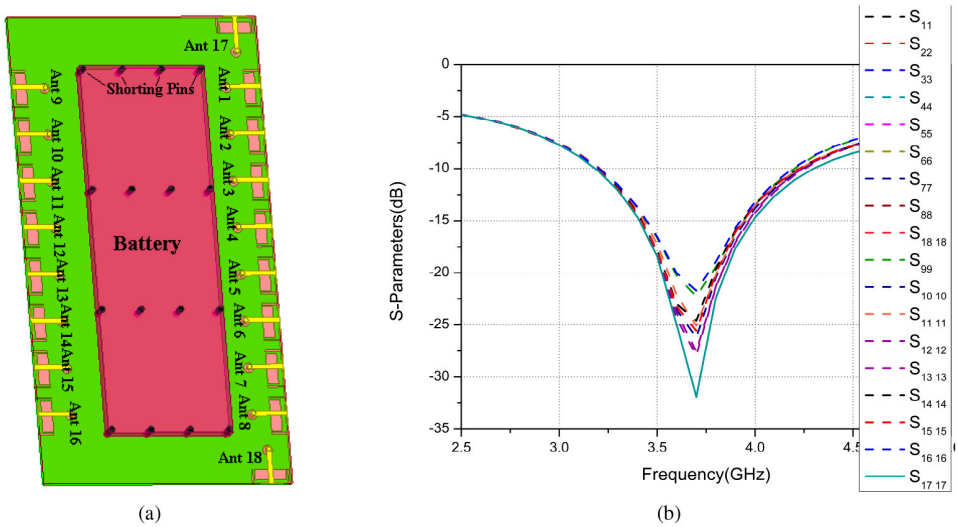

FIGURE 22. (a) Simulation model of the proposed antenna with battery (b) Simulated reflection coefficient values of the proposed antenna design integrated with battery.

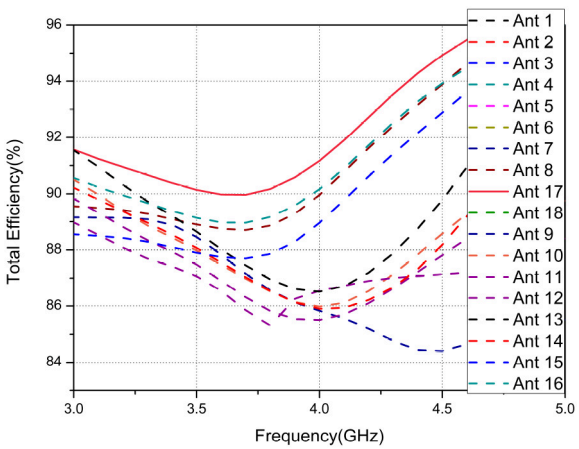

FIGURE 23. Simulated values of antenna efficiency of the proposed antenna design integrated with battery.

IV. CONCLUSION

In this work, an 18 element massive MIMO compatible antenna system consisting of slot antennas and open ended decoupling slots is introduced. The proposed MIMO antenna array has −10 dB bandwidth of more than 900 MHz that covers both LTE band 42 and LTE band 43. The antenna has a simple structure without any external decoupling mechanisms that gives the added advantage of ease of fabrication. The proposed design shows excellent performance with MIMO parameters like reduced mutual coupling (<20 dB), acceptable ECC (<0.01)and improved value of total efficiency (>87%). The peak ergodic channel capacity for proposed 18 × 18 MIMO antenna array (with 20 dB SNR) can attain a value as high as 704.34% then that of upper limit of 2 × 2 MIMO array. The proposed design could be considered as a good candidate in future 5G smartphones

REFERENCES

[1] W. Hong, "Solving the 5G mobile antenna puzzle: Assessing future directions for the 5G mobile antenna paradigm shift," *IEEE Microw. Mag.*, vol. 18, no. 7, pp. 86–102, Nov./Dec. 2017.

[2] S. Zhang, K. Zhao, Z. Ying, and S. He, "Adaptive quad-element multi-wideband antenna array for user-effective LTE MIMO mobile terminals," *IEEE Trans. Antennas Propag.*, vol. 61, no. 8, pp. 4275–4283, Aug. 2013.

[3] J. W. Wallace, M. A. Jensen, A. L. Swindlehurst, and B. D. Jeffs, "Experimental characterization of the MIMO wireless channel: Data acquisition and analysis," *IEEE Trans. Wireless Commun.*, vol. 2, no. 2, pp. 335–343, Mar. 2003.

[4] J. G. Andrews *et al.*, "What will 5G be?" *IEEE J. Sel. Areas Commun.*, vol. 32, no. 6, pp. 1065–1082, Jun. 2014.

[5] L. Zheng and D. N. C. Tse, "Diversity and multiplexing: A fundamental tradeoff in multiple-antenna channels," *IEEE Trans. Inf. Theory*, vol. 49, no. 5, pp. 1073–1096, May 2003.

[6] H. Xu *et al.*, "A compact and low-profile loop antenna with six resonant modes for LTE smartphone," *IEEE Trans. Antennas Propag.*, vol. 64, no. 9, pp. 3743–3751, Sep. 2016.

[7] S. Zhang, Z. Ying, J. Xiong, and S. He, "Ultrawideband mimo/diversity antennas with a tree-like structure to enhance wideband isolation," *IEEE Antennas Wireless Propag. Lett.*, vol. 8, pp. 1279–1282, 2009.

[8] J.-Y. Lee, S.-H. Kim, and J.-H. Jang, "Reduction of mutual coupling in planar multiple antenna by using 1-D EBG and SRR structures," *IEEE Trans. Antennas Propag.*, vol. 63, no. 9, pp. 4194–4198, Sep. 2015.

[9] Z. Li, Z. Du, M. Takahashi, K. Saito, and K. Ito, "Reducing mutual coupling of mimo antennas with parasitic elements for mobile terminals," *IEEE Trans. Antennas Propag.*, vol. 60, no. 2, pp. 473–481, Feb. 2012.

[10] S. Zhang, B. K. Lau, Y. Tan, Z. Ying, and S. He, "Mutual coupling reduction of two PIFAs with a *T*-shape slot impedance transformer for MIMO mobile terminals," *IEEE Trans. Antennas Propag.*, vol. 60, no. 3, pp. 1521–1531, Mar. 2012.

[11] Y.-L. Ban, C. Li, C.-Y.-D. Sim, G. Wu, and K.-L. Wong, "4G/5G multiple antennas for future multi-mode smartphone applications," *IEEE Access*, vol. 4, pp. 2981–2988, 2016.

[12] M. Alibakhshikenari *et al.*, "A comprehensive survey on various decoupling mechanisms with focus on metamaterial and metasurface principles applicable to SAR and MIMO antenna systems," *IEEE Access*, vol. 8, pp. 192965–193004, 2020.

[13] M. Alibakhshikenari, B. S. Virdee, and E. Limiti, "Study on isolation and radiation behaviours of a 34× 34 array-antennas based on SIW and metasurface properties for applications in terahertz band over 125–300 Ghz," *Optik*, vol. 206, Mar. 2020, Art. no. 163222.

[14] M. Alibakhshikenari *et al.*, "Isolation enhancement of densely packed array antennas with periodic MTM-photonic bandgap for SAR and MIMO systems," *IET Microw. Antennas Propag.*, vol. 14, no. 3, pp. 183–188, 2019.

[15] M. Alibakhshikenari, M. Khalily, B. S. Virdee, C. H. See, R. A. Abd-Alhameed, and E. Limiti, "Mutual-coupling isolation using embedded metamaterial EM bandgap decoupling slab for densely packed array antennas," *IEEE Access*, vol. 7, pp. 51827–51840, 2019.

[16] K.-L. Wong, C.-Y. Tsai, and J.-Y. Lu, "Two asymmetrically mirrored gap-coupled loop antennas as a compact building block for eight-antenna MIMO array in the future smartphone," *IEEE Trans. Antennas Propag.*, vol. 65, no. 4, pp. 1765–1778, Apr. 2017.

[17] K.-L. Wong, B.-W. Lin, and B. W.-Y. Li, "Dual-band dual inverted-F/loop antennas as a compact decoupled building block for forming eight 3.5/5.8-Ghz MIMO antennas in the future smartphone," *Microw. Opt. Technol. Lett.*, vol. 59, no. 11, pp. 2715–2721, 2017.

[18] A. Zhao and Z. Ren, "Size reduction of self-isolated MIMO antenna system for 5G mobile phone applications," *IEEE Antennas Wireless Propag. Lett.*, vol. 18, no. 1, pp. 152–156, Jan. 2019.

[19] L. Sun, H. Feng, Y. Li, and Z. Zhang, "Compact 5G MIMO mobile phone antennas with tightly arranged orthogonal-mode pairs," *IEEE Trans. Antennas Propag.*, vol. 66, no. 11, pp. 6364–6369, Nov. 2018.

[20] X. Ling and R. Li, "A novel dual-band MIMO antenna array with low mutual coupling for portable wireless devices," *IEEE Antennas Wireless Propag. Lett.*, vol. 10, pp. 1039–1042, 2011.

[21] A. A. Al-Hadi, J. Ilvonen, R. Valkonen, and V. Viikari, "Eight-element antenna array for diversity and MIMO mobile terminal in LTE 3500 MHz band," *Microw. Opt. Technol. Lett.*, vol. 56, no. 6, pp. 1323–1327, 2014.

[22] K.-L. Wong and J.-Y. Lu, "3.6-Ghz 10-antenna array for MIMO operation in the smartphone," *Microw. Opt. Technol. Lett.*, vol. 57, no. 7, pp. 1699–1704, 2015.

[23] M.-Y. Li *et al.*, "Eight-port orthogonally dual-polarized antenna array for 5G smartphone applications," *IEEE Trans. Antennas Propag.*, vol. 64, no. 9, pp. 3820–3830, Sep. 2016.

[24] Z. Zhang, *Antenna Design for Mobile Devices*. Hoboken, NJ, USA: Wiley, 2017.

[25] M. S. Sharawi, A. T. Hassan, and M. U. Khan, "Correlation coefficient calculations for MIMO antenna systems: A comparative study," *Int. J. Microw. Wireless Technol.*, vol. 9, no. 10, pp. 1991–2004, 2017.

[26] M. S. Sharawi, "Printed multi-band MIMO antenna systems and their performance metrics [wireless corner]," *IEEE Antennas Propag. Mag.*, vol. 55, no. 5, pp. 218–232, Oct. 2013.

[27] R. Tian, B. K. Lau, and Z. Ying, "Multiplexing efficiency of MIMO antennas," *IEEE Antennas Wireless Propag. Lett.*, vol. 10, pp. 183–186, 2011.

[28] Y. Li, C.-Y.-D. Sim, Y. Luo, and G. Yang, "High-isolation 3.5 Ghz eight-antenna MIMO array using balanced open-slot antenna element for 5G smartphones," *IEEE Trans. Antennas Propag.*, vol. 67, no. 6, pp. 3820–3830, Jun. 2019.

[29] Z. Ren, A. Zhao, and S. Wu, "MIMO antenna with compact decoupled antenna pairs for 5G mobile terminals," *IEEE Antennas Wireless Propag. Lett.*, vol. 18, no. 7, pp. 1367–1371, Jul. 2019.

[30] A. Ren, Y. Liu, and C.-Y.-D. Sim, "A compact building block with two shared-aperture antennas for eight-antenna MIMO array in metal-rimmed smartphone," *IEEE Trans. Antennas Propag.*, vol. 67, no. 10, pp. 6430–6438, Oct. 2019.

[31] L. Chang, Y. Yu, K. Wei, and H. Wang, "Polarization-orthogonal co-frequency dual antenna pair suitable for 5G MIMO smartphone with metallic bezels," *IEEE Trans. Antennas Propag.*, vol. 67, no. 8, pp. 5212–5220, Aug. 2019.

[32] K.-L. Wong, J.-Y. Lu, L.-Y. Chen, W.-Y. Li, and Y.-L. Ban, "8-antenna and 16-antenna arrays using the quad-antenna linear array as a building block for the 3.5-Ghz LTE MIMO operation in the smartphone," *Microw. Opt. Technol. Lett.*, vol. 58, no. 1, pp. 174–181, 2016.

NAVEEN JAGLAN was born in 1989. He received the B.Tech. (Hons.) and M.Tech. (Hons.) degrees in electronics and communication engineering from Kurukshetra University, Kurukshetra, India, in 2009 and 2011, respectively, and the Ph.D. degree on "Design and Development of Microstrip Antennas Integrated with Electromagnetic Band Gap Structures" from the Jaypee Institute of Information Technology, Noida, India, in June 2017. He has authored/coauthored several research papers in referred international journals and conferences. His research has included microwave communications, 5G antenna design, planar and conformal microstrip antennas, including array mutual coupling, artificial materials (metamorphic, metamaterials), EBG, PBG, FSS, DGS, novel antennas, UWB antennas, MIMO systems, numerical methods in electromagnetic, composite right/left handed transmissions and high-k dielectrics. His skill includes modeling of antenna and RF circuits with ansoft HFSS/CST microwave studio/ADS momentum, measurements using vector network analyzer and anechoic chamber.

SAMIR DEV GUPTA received the B.E. degree in electronics from the University Visvesvaraya College of Engineering, Bangalore University, Bengaluru, the M.Tech. degree in electrical engineering from IIT Madras, the M.Sc. degree in defence studies from Madras University, and the Ph.D. degree from JIIT Noida. He is currently designated as the Director and an Academic Head of the Jaypee University of Information Technology (JUIT), Waknaghat, India. He has over three and a half decades of work experience in the areas of avionics, communication, radar systems and teaching at UG and PG level. His teaching career spans over 22 years and six months includes in addition to teaching with JIIT, Noida, since December 2002 and the Institute of Armament Technology, Pune University, currently with the Defence Institute of Advanced Technology (Deemed University) for PG programmes and training and development needs of Indian Air Force (IAF) and Defence Research and Development Organization (DRDO), Air Force Technical College (AFTC), Bengaluru, where graduate engineers from IIT's, NIT's, and Indian and foreign Universities undergo aeronautical engineering (electronics) course for about 18 months prior joining Technical Officers' Branch, IAF, and Advanced Stage Trade Training Wing with Guided Weapon Training Institute, Baroda. He was also a recognized Postgraduate Teacher of Microwave Communication with Pune University. His previous assignments includes, the Deputy Director at Air Headquarters and were involved in planning, coordinating and directing maintenance, modification of aircraft and helicopter systems, modifications and induction of advance electronic systems into IAF, a Commanding Officer of an 8 GHz LOS microwave communication unit, a Senior Engineer looking after maintenance of airfield navigation aids, techno-logistic management of ground-based communication equipment as Aeronautical Engineering (Electronics) Branch officer, IAF, the Chairman Communication Advisory Committee, IAT, Pune. He is qualified for first and second line servicing of Mirage-2000 aircraft. Work experience on Mirage Mission Simulator and fly by wire systems of Mirage-2000 aircraft. Led and supervised highly qualified and skilled engineering officers and technicians of IAF in maintenance and operation of missile, radar, and communication systems. Experienced in management of resources to achieve time bound targets and objectives viz. Successfully implemented contract with international and national agencies for induction of unmanned aerial vehicle, portable laser designating systems and up gradation of aircraft simulators for the IAF. Prior to joining JUIT, as the Director and an Academic Head, he was a Professor with the Department of ECE, JIIT, where he also initiated training and placement process. Successfully placed first and second batch students of Jaypee Education System in top-notch national and multinational organizations through campus recruitment. He has been associated with JIIT in students' welfare and discipline as an Associate Dean of Students and Chairman Proctorial Board. His publications in referred journals and conferences are well cited. His research interest is in the area of conformal microstrip patch antenna for aircraft systems.

MOHAMMAD S. SHARAWI (Senior Member, IEEE) is a Professor of Electrical Engineering with Polytechnique Montréal, Montréal, QC, Canada, where he is also a Member of the Poly-Grames Research Center. He was with the King Fahd University of Petroleum and Minerals (KFUPM), Saudi Arabia, from 2009 to 2018, where he founded and directed the Antennas and Microwave Structure Design Laboratory. He was a Visiting Professor with the Intelligent Radio (iRadio) Laboratory, Electrical Engineering Department, University of Calgary, Alberta, Canada, during the Summer-Fall 2014. He was a Visiting Research Professor with Oakland University during the summer 2013. He has more than 300 papers published in refereed journals and international conferences, ten book chapters, one single authored book entitled *Printed MIMO Antenna Engineering* (Artech House, 2014), and the Lead Author of the recent book *Design and Applications of Active Integrated Antennas* (Artech House, 2018). He has 25 issued and 12 pending patents in the U.S. Patent Office. His areas of research include multiband printed multiple-input-multiple-output (MIMO) antenna systems, reconfigurable and active integrated antennas, applied electromagnetics, millimeter-wave MIMO antennas and integrated 4G/5G antennas for wireless handsets, and access points. He served on the Technical and organizational program committees of several international conferences, such as EuCAP, APS, IMWS-5G, APCAP, and iWAT. He is serving as an Associate Editor for the IEEE ANTENNAS AND WIRELESS PROPAGATION LETTERS and *IET Microwaves, Antennas and Propagation*, and an Area Editor for *Microwave and Optical Technology Letters* (Wiley). He is the Specialty Editor of the newly launched *Frontiers in Communications and Networks*, the System and Test-Bed design section.